Unfolding Pathway of a Globular Protein by Surfactants Monitored with Raman Optical Activity

ARTICLE *in* JOURNAL OF PHYSICAL CHEMISTRY LETTERS · JANUARY 2014

Impact Factor: 7.46

6 AUTHORS, INCLUDING:

Jose Hierrezuelo

Dublin City University

28 PUBLICATIONS **335** CITATIONS

SEE PROFILE

Juan Teodomiro López Navarrete

University of Malaga

335 PUBLICATIONS **5,253** CITATIONS

SEE PROFILE

Juan Casado

University of Malaga

227 PUBLICATIONS **3,690** CITATIONS

SEE PROFILE

Francisco Javier Ramírez

University of Malaga

121 PUBLICATIONS **1,687** CITATIONS

SEE PROFILE

THE JOURNAL OF PHYSICAL CHEMISTRY Letters

Letter

pubs.acs.org/JPCL

Unfolding Pathway of a Globular Protein by Surfactants Monitored with Raman Optical Activity

Belén Nieto-Ortega,[†] José M. Hierrezuelo,[‡] Cristóbal Carnero Ruiz,[‡] Juan Teodomiro López Navarrete,[†] Juan Casado,[†] and Francisco J. Ramírez*[,†]

[†]Department of Physical Chemistry, Faculty of Sciences and [‡]Department of Applied Physics II, Engineering School, University of Málaga, 29071 Málaga, Spain

Supporting Information

ABSTRACT: Protein denaturation by surfactants has received increased attention in the last years due to its implications in topics such as pharmaceutics, cosmetics, paints, or biotechnology. This phenomenon is highly dependent on the physicochemical (structural) properties of the denaturing agents. In this work, we have measured for the first time the Raman optical activity (ROA) of bovine serum albumin (BSA) in the presence of three surfactants (anionic, cationic, and neutral), which has allowed us to detect new spectroscopic insights of the protein−surfactant interaction that conventional Raman spectroscopy cannot. Our work proposes two new groups of ROA marker bands to explore the unfolding of BSA induced by surfactants, which are related to "polar" (amide I and III modes) and "apolar" (methylene bending and phenyl breathing modes) protein sections. The appearance of the former groups is related to the initial attack of the surfactant, while the second groups relate to the hydrophobic unfolding.

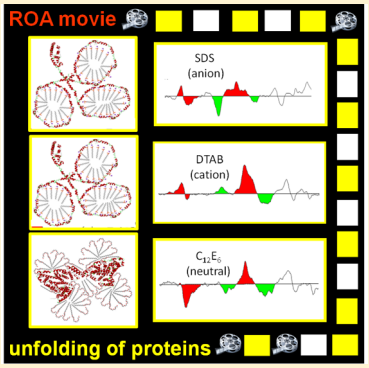

SECTION: Biophysical Chemistry and Biomolecules

The general principles of folding onto the native forms of proteins (biologically active conformations) are encoded in the amino acid sequence or primary structure of the protein. For decades, scientists have made considerable efforts in elucidating these codes by means of a wide catalogue of in vitro experiments and more recently also by utilizing in silico approaches. Traditionally, most of the studies of protein folding in solution are based on the exploration of the induced denaturation of the protein from its native form. Different agents can induce this denaturation, pH, temperature, heavy metals, ionic strength, chemicals, and so forth. In the past few years, surfactants have received increased attention[1,2] as denaturation agents given their relevance in topics such as pharmaceutics, cosmetics, paints, biotechnology, coatings, and so forth.[3−5] Structurally, a surfactant is an amphipathic molecule with a hydrophobic residue decorated with a hydrophilic head bearing an electric charge that determines its anionic (cationic) or nonionic (neutral) character. In aqueous solutions, these amphipathic molecules form micelles above a critical concentration (critical micelle concentration or cmc).

The mechanism of interaction between surfactants and globular proteins is well-established.[3,6−8] From this topic, surfactants can be divided into two main groups, those that are directly bounded to particular protein sites where the unfolding is initiated and those that are bounded to sites of the protein that do not destroy the tertiary structure. Anionic surfactants belong to the former case and act by a first attack to the outermost cationic residues in the surface (i.e., the side chains of lysyl, histidyl, and arginyl residues) followed by protein unfolding that unburies the internal hydrophobic protein part, becoming accessible to the surfactant alkyl tails that complete the unfolding. In the case of the nonionic surfactants, the first hydrophilic attack does not take place, and the surfactants only attack the hydrophobic side chains at the protein surface.[6,9]

A well-established method to study the structure of proteins in aqueous solutions is the use of electronic circular dichroism (ECD),[10] a chiroptical technique that has been applied for decades to elucidate the structure and function of a wide range of biological molecules including proteins,[10−13] carbohydrates,[14−19] nucleic acids,[20−22] and even more complex structures as viruses.[23−26] Nevertheless, the ECD spectra provide limited structural information because of the scarce number of electronic bands. On the contrary, vibrational spectroscopy provides us with rich spectra and well-structured bands that can be directly assigned to specific molecular sites or domains, giving us a high-resolution spectroscopic structural fingerprint. Here, Raman optical activity, abbreviated as ROA, the Raman branch of the chiroptical vibrational spectroscopy, emerged as a powerful tool for structural studies of chiral molecules and supramolecular assemblies in *in vivo* media.[27−32] Compared with conventional Raman spectroscopy, ROA offers much higher selectivity and sensitivity because it is not interfered with by achiral molecules and is able to detect

Received: October 23, 2013
Accepted: December 2, 2013

   dx.doi.org/10.1021/jz402291s | *J. Phys. Chem. Lett.* 2014, 5, 8−13

features associated with the chiroptically active environments. Since the first report of the ROA spectrum of a protein in 1990,[33] its application to the study of biomolecules has represented by large the most exciting structural application, although other applications are recently entering the scene.[34−38]

Nowadays, many reports of ROA spectra of model proteins and polypeptides have been described, and their ROA signatures have been closely related with their known secondary structures,[39,40] a topic in rapid expansion as more ROA facilities are available. To further progress in this direction, we report here the ROA signature of the interaction between a well-known protein, bovine serum albumin (BSA), and surfactants pursuing to obtain new spectroscopic−structure pieces of information about the unfolding of the protein. BSA is one of the best known proteins, and its ROA spectrum was reported in 1994.[41] The native form of BSA is a well-structured helix, with an α-helix content of around 67% and turns and loops forms representing the remaining protein backbone with a large number of disulfide bridges.[42] The interactions of BSA with a variety of ligands, including fatty acids, amino acids, drugs metals, and surfactants, have been widely analyzed by different physicochemical techniques including Raman spectroscopy.[43,44] In this Letter, we have studied the interaction of BSA with three selected surfactants that share the dodecyl chain as the hydrophobic moiety in the forms of anionic sodium dodecyl sulfate, cationic dodecyl trimethyl ammonium bromide, and neutral hexaethylene glycol monododecyl ether. With this choice, the initial surfactant−protein bonding takes place through the hydrophilic heads. For each surfactant−protein ensemble, we have examined a range of surfactant concentrations covering the pre- and postmicellar regions. The purpose of our work is to report the ROA spectra of the BSA protein during the different steps of its denaturation or unfolding process by the attack of surfactants.

The simultaneously recorded Raman and ROA spectra of BSA in the presence of the surfactants are displayed in Figures 1−3. Three surfactant concentrations were selected in each case to cover the regions below the cmc, slightly above the cmc, and well above the cmc. The Raman spectra of the surfactants in the absence of protein (see Figures S1−S3 of the Supporting Information (SI)) do not show any peaks that noticeably interfere with the main protein marker bands. Relevant structural information can be inferred from the BSA Raman band at 1558 cm^{-1}. It is known as W3 and is assigned to a stretching vibration of the indole ring in the tryptophan side chains.[45] The intensity of this band decreases upon SDS addition until the final disappearance at high concentrations of SDS (see Figure S5, SI). This result agrees with the knowledge that the initial step of the protein−ligand interaction goes by bonding through the tryptophan residues to which the W3 indole charged ring band is due.[46] A similar trend is observed for DTBA, which is consistent with the neutral character of this amino acid. The bands at 1340 and 1323 cm^{-1}, two amide III modes,[47] are also altered in the same way by the addition of the two charged surfactants; the intensity of the band at 1340 cm^{-1} decreases while that at 1323 cm^{-1} increases. These bands are considered as markers of the secondary structure of the protein,[14] the α-helix band at 1340 cm^{-1} and the random coil at 1323 cm^{-1}. The Raman spectra of the BSA-$C_{12}E_6$ solutions exhibit fewer changes than those of the ionic surfactants. The most noticeable feature is the weakening of the W3 Raman band at 1558 cm^{-1} (see Figure S4 (SI) for more details).

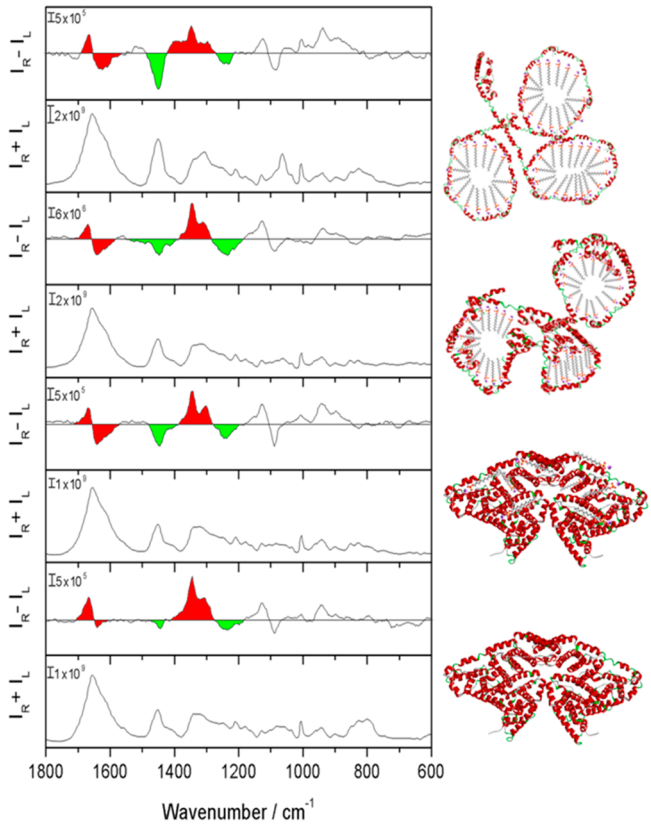

Figure 1. Backscattered Raman and ROA spectra of BSA in the native form (bottom pair), BSA with SDS 2 mM (second pair), BSA with SDS 20 mM (third pair), and BSA with SDS 50 mM (top pair). The BSA concentration is 50 mg/mL in all solutions. The most relevant ROA features have been colored (red: amide I and amide III; green: hydrophobic moieties). Corresponding schemes of the BSA−SDS interaction at each step are displayed for better understanding.

Before discussing the ROA spectra of BSA in the presence of SDS, it is worthwhile to review the general features of the ROA spectrum of a protein.[39] First, the 1700−1630 cm^{-1} region is dominated by the amide I mode, which arises from the stretching vibrations of the C═O groups involved in the hydrogen bonding network sustaining the helicoidal structures. Second, the 1350−1230 cm^{-1} region is dominated by the amide III mode arising from C_α−N stretching and N−H bending vibrations, whose ROA appearance is closely related with the protein secondary structure, in particular, with α-helix and β-type substructures. These bands can be stated as arising from the more polar environment of the protein. Finally, the 1150−870 cm^{-1} region exhibits the peptide backbone vibrations, and therefore, their associated ROA bands are influenced also by the protein secondary structure.

Concerning the BSA−SDS ROA spectra, a general feature is their more structured aspect compared to the spectrum of the native form. Free native proteins usually present highly dynamic structures in which the continuous conformational movements avoid the vibrational ROA features to exhibit well-defined shapes and, in contrast, display poorly structured spectra. As a result of the interaction with SDS, the protein structure gets more rigid, its internal bond angles, responsible for the conformational freedom, become stiffened, and the ROA spectrum becomes much more defined.[47,48]

Going into more particular details, the main ROA features observed upon SDS addition are as follows: (i) The amide I

dx.doi.org/10.1021/jz402291s | J. Phys. Chem. Lett. 2014, 5, 8−13

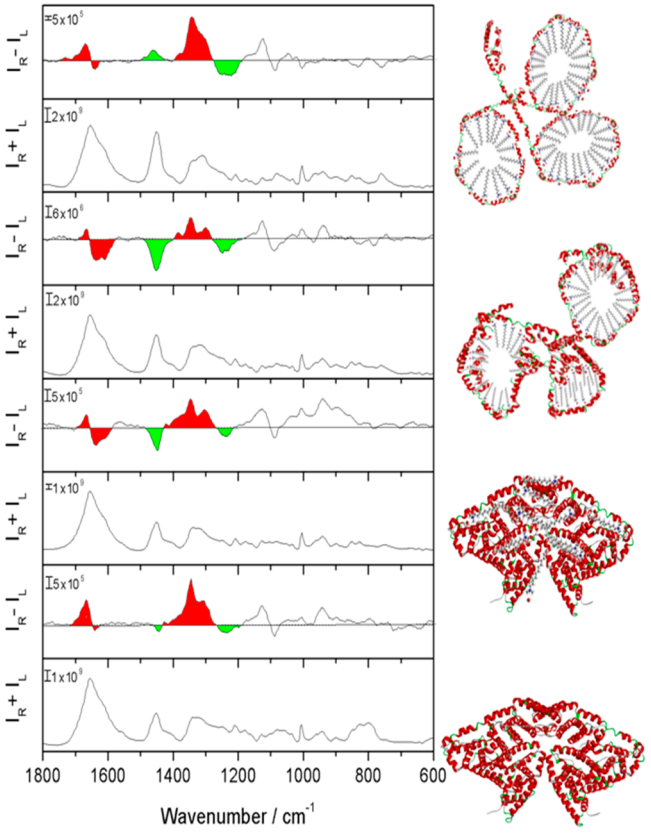

Figure 2. Backscattered Raman and ROA spectra of BSA in the native form (bottom pair), BSA with DTAB 5 mM (second pair), BSA with DTAB 20 mM (third pair), and BSA with DTAB 50 mM (top pair). The BSA concentration is 50 mg/mL in all solutions. The most relevant ROA features have been colored (red: amide I and amide III; green: hydrophobic moieties). Corresponding schemes of the BSA–DTAB interaction at each step are displayed for better understanding.

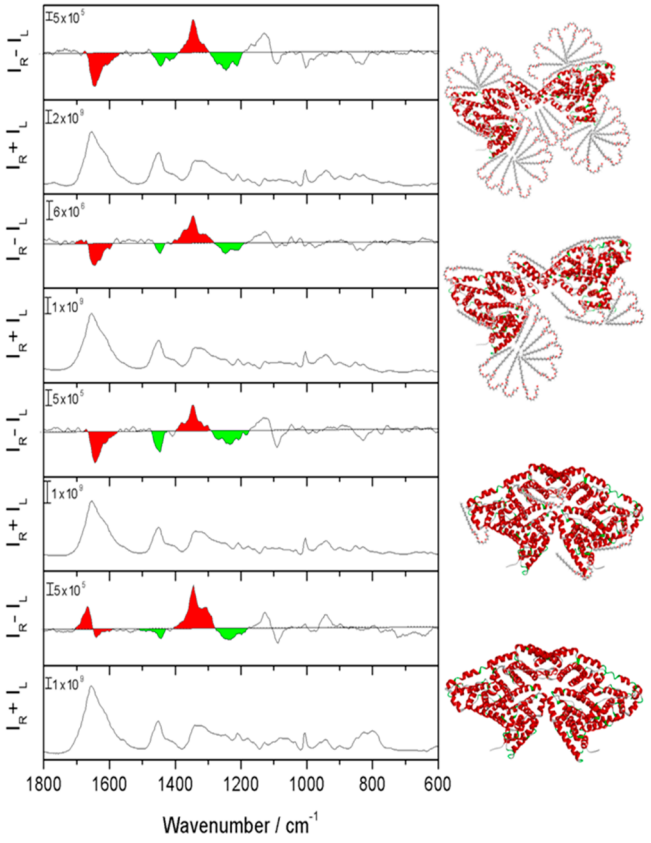

Figure 3. Backscattered Raman and ROA spectra of BSA in the native form (bottom pair), BSA with $C_{12}E_6$ 0.2 mM (second pair), BSA with $C_{12}E_6$ 5 mM (third pair), and BSA with $C_{12}E_6$ 10 mM (top pair). The BSA concentration is 50 mg/mL in all solutions. The most relevant ROA features have been colored (red: amide I and amide III; green: hydrophobic moieties). Corresponding schemes of the BSA–$C_{12}E_6$ interaction at each step are displayed for better understanding.

bisignate band at +1666/−1639 cm^{-1} remains invariant. This band was first proposed by Barron et al.[30,41] and later confirmed in the ROA spectrum of poly(L-lysine) as a spectroscopic marker of the α-helix conformation.[48] The behavior of this amide I band in our BSA–SDS solutions would indicate that the surfactant does not significantly alter the portion of the α-helix conformation in the BSA secondary structure. (ii) The weak negative band at 1450 cm^{-1} arises from bending vibrations of the CH_2 and CH_3 aliphatic groups and becomes stronger and sharper together with the appearance of two new weak negative ROA bands at 1246 and 1227 cm^{-1}. The intensification of the negative band at 1450 cm^{-1} is evidence of the changes in the aliphatic side chain conformation similar to those reported for disordered poly(L-lysine), while the two new negative weak bands measured at 1246 and 1227 cm^{-1} suggest the formation of some β-type structures.[49,50] Finally, (iii) the intensity of the band at 1308 cm^{-1} is enhanced (relative to the band at 1346 cm^{-1}) and its frequency shifted to 1296 cm^{-1} in the spectrum of the solution at 50 mM of SDS. These bands, which are assigned to the amide III mode of the peptide bond, have been related with different forms of the α-helix that are strongly related with the folding imposed by the tertiary structure of the protein. Hence, the band at 1308 cm^{-1} arises from hidden nonhydrated α sequences, while the band at 1346 cm^{-1} is assigned to water-exposed or hydrated α domains.[51] The changes indicate that the nonhydrated domains, or hydrophobic sites (α-helix band at 1308 cm^{-1}), of the protein are transformed by exposure to the SDS surfactant while the hydrophilic part (α-helix band at 1346 cm^{-1}), already exposed to water, does not change much with the SDS addition. This result is then fully compatible with the interaction steps described in the literature for the union between SDS and globular proteins.

The action of cationic surfactants has received less attention than their anionic parents possibly because their interaction with globular proteins seems to exhibit similar characteristics. Figure 2 shows the ROA spectra of BSA in the presence of DTAB at the same concentrations as SDS. At a first glance, the main ROA features can be directly correlated with those already described for SDS. However, interesting differences are detected when comparing the ROA spectra of BSA with the anionic and the cationic surfactants at saturation regimes; (i) a new positive ROA band at 1385 cm^{-1} is measured only for DTAB, (ii) the negative band at 1450 cm^{-1} of the CH_2/CH_3 bending vibrations of BSA with SDS is now positive with DTAB and shifts upward by 10 cm^{-1}, and (iii) the positive band at 1006 cm^{-1}, due to a breathing mode of phenyl residues, which is invariant for the BSA–SDS solutions, is transformed into a negative peak for BSA–DTAB.

In energetic terms, the main difference between the interaction of cationic and anionic surfactants with globular proteins concerns the enthalpy change, which is negative for

dx.doi.org/10.1021/jz402291s | J. Phys. Chem. Lett. 2014, 5, 8–13

anionic and positive for cationic.[52] In both cases, the total enthalpy results from two opposite contributions, the binding enthalpy, which is always negative, and the unfolding component, which is always positive. As a consequence of these counteracting effects, the value of the variation of enthalpy for the surfactant−protein interaction is often small compared with the large entropy increase, which is the driving force of the whole process at room temperature. The origin of the large ΔS values is the hydrophobic interaction, which releases water molecules into the solvent into a more disordered state than within the protein structure. As an interesting example, the interaction between SDS and ovalbumin occurs without a measurable enthalpy change at 25 °C ($\Delta G \approx T\Delta S$).[53] Assuming that the hydrophobic attractions drive the interaction of the globular protein with a cationic surfactant and that the interactions with an anionic surfactant could be, in principle, also conducted by enthalpy, we should then be able to relate the changes between the BSA−SDS and BSA−DTAB ROA spectra with structural effects that originated from these two mechanisms of unfolding. This can be found in the sign inversion and wavenumber shift of the BSA bands at 1450 and 1006 cm^{-1} in the presence of DTAB. As already described, they are assigned to vibrations of the hydrophobic groups, in particular, that at 1450 cm^{-1} to bending modes of the CH_2/CH_3 groups, which are widely present in the main target residues of the cationic surfactants (i.e., the side chains of glutamic and aspartic acids) as well as the hydrophobic phenyl residues whose breathing modes originate in the ROA band at 1006 cm^{-1}. By large, these "hydrophobic" ROA bands reveal the hydrophobic entropy-driven attack of DTAB to BSA in contrast with the unfolding process with SDS. To our knowledge, these spectroscopic−structure connections based on the ROA fingerprint and related with the surfactant mechanism of protein unfolding have not been reported until now.

Nonionic surfactants are often used to prevent or minimize protein aggregation in processes such as fermentation, purification, freeze-drying, or storage. It has been well-established that they preserve the structure of proteins as they mainly interact by means of their hydrophobic exterior part, not appreciably disturbing the protein secondary structure. Figure 3 displays the ROA spectra of BSA in the presence of three different concentrations of $C_{12}E_6$, as a model of a neutral surfactant. Considering the low cmc of this neutral surfactant, around 0.1 mM, and in order to record well-resolved and interpretable ROA spectra, the three concentrations studied here are above the cmc threshold.

The ROA spectra of the BSA−$C_{12}E_6$ solutions show some distinctive features regarding those observed in the two previously discussed ionic surfactants. Negligible changes on the 1660 and 1300−1350 cm^{-1} amide ROA bands are observed during the addition of the surfactant. The interaction with $C_{12}E_6$ gives rise to two new negative ROA bands at 1245 and 1212 cm^{-1}, while that at 1006 cm^{-1}, due to the phenyl breathing vibrations of the side chain, undergoes a sign inversion similar to that observed after BSA interaction with the DTAB cationic surfactant. In marked contrast with the above similitude with DTAB, the sign of the ROA marker band due to bending vibrations of the CH_2/CH_3 aliphatic side chain at 1450 cm^{-1} is preserved, which reveals the same behavior to that observed with the SDS anionic surfactant. In summary, the ROA spectra of BSA in the presence of the neutral uncharged $C_{12}E_6$ surfactant are consistent with a hydrophobic scenario that is common to the three types of surfactant independent of the charge, which only makes a difference in the initial events of the surfactant attack.

This work represents the first application of ROA to follow the process of the interaction of a protein with surfactants, in this case, a globular protein. We have reported the ability of ROA spectroscopy to detect many more spectroscopic details than conventional Raman spectroscopy does in *in vivo* media. In this way, the ROA spectra provide key new spectral features, unreported until now. These are (i) the two ROA features in the 1600 and 1300−1350 cm^{-1} ranges emerging from vibrational modes of the amide groups of the peptide bond environment or embedded in a polar framework and related with the existence of α-helical forms and that have been correlated with the opening of the protein structure in the initial steps of the unfolding induced exclusively by ionic surfactants and (ii) the methyl and methylene bending modes at 1450 cm^{-1} together with the band close to 1000 cm^{-1} of the phenyl breathing modes, which are both vibrations placed in the most apolar fraction of the protein and that from a mechanistic point of view are especially sensitive to the unfolding mode by the cationic surfactant, less studied than the anionic ones. Nonetheless, these ROA apolar features depict the unique hydrophobic scenario for the attack of BSA by the neutral surfactant. We then demonstrated the ability of ROA in structural and mechanistic studies of proteins in close to or *in vivo* conditions. This study might open the way for new applications of ROA spectroscopy, in many aspects still in its infancy, in protein structural chemistry and in protein mechanistic studies.

■ ASSOCIATED CONTENT

Supporting Information

Experimental methods, definition of the tryptophan torsion angles in the tryptophan structure, Raman spectra of BSA in solution with the different surfactants and extended Raman and ROA spectra until 200 cm^{-1}. See DOI: 10.1039/b000000x/. This material is available free of charge via the Internet at http://pubs.acs.org.

■ AUTHOR INFORMATION

Corresponding Author

*E-mail: ramirez@uma.es.

Notes

The authors declare no competing financial interest.

■ ACKNOWLEDGMENTS

This work was supported by the Ministerio de Educación (project CTQ2012-33733) and Junta de Andalucía (Project P09-FQM-4708), and B.N.-O is indebted to MEC for her FPU studentship (Grant No. AP2009-2797).

■ REFERENCES

(1) Otzen, D. E.; Sehgal, P.; Westh, P. α-Lactalbumin is Unfolded by all Classes of Surfactants but by Different Mechanisms. *J. Colloid Interface Sci.* **2009**, *329*, 273−283.

(2) Andersen, K. K.; Otzen, D. E. How Chain Length and Charge Affect Surfactant Denaturation of Acyl Coenzyme A Binding Protein (ACBP). *J. Phys. Chem. B* **2009**, *113*, 13942−13952.

(3) Steinhardt, J.; Reynolds, J. A. *Multiple Equilibria in Proteins*; Academic Press: New York, 1969.

(4) Burkhard, R. K.; Stolzenberg, G. E. Interaction between Sodium Dodecyl Sulfate and Ferricytochrome. *Biochemistry* **1972**, *11*, 1672−1677.
(5) Goddard, E. D. Polymer Surfactant Interaction 2. Polymer and Surfactant of Opposite Charge. *Colloids Surf.* **1986**, *19*, 301−329.
(6) Jones, M. N. Surfactant Interactions with Biomembranes and Proteins. *Chem. Soc. Rev.* **1992**, *21*, 127−136.
(7) Jones, M. N. A Theoretical Approach to the Binding of Amphipathic Molecules to Globular Proteins. *Biochem. J.* **1975**, *151*, 109−114.
(8) Agre, P.; Parker, J. C. *Red Blood Cell Membranes: Structure, Function, Clinical Implications*; CRC Press: New York, 1989.
(9) Jones, M. N. *Biological Interfaces: An Introduction to the Surface and Colloid Science of Biochemical and Biological Systems*; Elsevier: Amsterdam, The Netherlands, 1975.
(10) Berova, N.; Polavarapu, P. L.; Nakanishi, K.; Woody, R. W. *Electronic Circular Dichroism of Proteins*; John Wiley & Sons, Inc.: Hoboken, NJ, 2012.
(11) Dang, Z.; Hirst, J. D. *Circular Dichroism in Protein Analysis*; Wiley-VCH: Weinheim, Germany, 2006.
(12) Harada, N.; Nakanishi, K.; Berova, N. *Electronic CD Exciton Chirality Method: Principles and Applications*; John Wiley & Sons, Inc.: Hoboken, NJ, 2012.
(13) Greenfield, N. J.; Fasman, G. D. Computed Circular Dichroism Spectra for the Evaluation of Protein Conformation. *Biochemistry* **1969**, *8*, 4108−4116.
(14) Purdie, N. *Circular Dichroism and the Conformational Analysis of Biomolecules*; Plenum Press: New York, 1996.
(15) Bose, P. K.; Polavarapu, P. L. Vibrational Circular Dichroism is a Sensitive Probe of the Glycosidic Linkage: α-Oligosaccharides of Glucose. *J. Am. Chem. Soc.* **1999**, *121*, 6094−6095.
(16) Bush, C. A.; Ralapati, S. *Vacuum UV Circular Dichroism Spectroscopy of Acetamido Sugars*; American Chemistry Society: New York, 1981.
(17) Hu, X.-J.; Wang, X.-B.; Kong, L.-Y. α-Glucosidase Inhibitors via Green Pathway: Biotransformation for Bicoumarins Catalyzed by Momordica Charantia Peroxidase. *J. Agric. Food Chem.* **1981**, *61*, 1501−1508.
(18) Gekko, K.; Matsuo, K. Vacuum-Ultraviolet Circular Dichroism Analysis of Biomolecules. *Chirality* **2006**, *18*, 329−334.
(19) Taniguchi, T.; Monde, K. *Optical Rotation, Electronic Circular Dichroism, and Vibrational Circular Dichroism of Carbohydrates and Glycoconjugates*; John Wiley & Sons, Inc.: Hoboken, NJ, 2012.
(20) Charney, E.; Yamaoka, K. Electric Dichroism of DNA in Aqueous Solutions: Electric Field Dependence. *Biochemistry* **1982**, *21*, 834−842.
(21) Yamaoka, K.; Charney, E. Electric Dichroism Studies of Macromolecules in Solutions. II. Measurements of Linear Dichroism and Birefringence of Deoxyribonucleic Acid in Orienting Electric Fields. *Macromolecules* **1973**, *6*, 66−76.
(22) Fasman, G. D.; Valenzuela, M. S.; Adler, A. J. Complexes of Deoxyribonucleic Acid with Fragments of Lysine-Rich Histone (f-1). Circular Dichroism Studies. *Biochemistry* **1971**, *10*, 3795−3801.
(23) Kostrikis, L. G.; Liu, D. J.; Day, L. A. Ultraviolet Absorbance and Circular Dichroism of Pf1 Virus: Nucleotide/Subunit Ratio of Unity, Hyperchromic Tyrosines and DNA bases, and High Helicity in the Subunits. *Biochemistry* **1994**, *33*, 1694−1703.
(24) Arnold, G. E.; Day, L. A.; Dunker, A. K. Tryptophan Contributions to the Unusual Circular Dichroism of fd Bacteriophage. *Biochemistry* **1992**, *31*, 7948−7956.
(25) Casadevall, A.; Day, L. A. Thermal Difference Circular Dichroism of Pf1 Filamentous Virus and Effects of Mercury(II), Silver(I), and Copper(II). *Biochemistry* **1988**, *27*, 3599−3602.
(26) Blanch, E. W.; Bell, A. F.; Hecht, L.; Day, L. A.; Barron, L. D. Raman Optical Activity of Filamentous Bacteriophages: Hydration of α-Helices. *J. Mol. Biol.* **1999**, *290*, 1−7.
(27) Uversky, V. N. Natively Unfolded Proteins: A Point Where Biology Waits for Physics. *Protein Sci.* **2002**, *11*, 739−756.
(28) Dunker, A. K.; Brown, C. J.; Lawson, J. D.; Iakoucheva, L. M.; Obradović, Z. Intrinsic Disorder and Protein Function. *Biochemistry* **2002**, *41*, 6573−6582.
(29) Barron, L. D.; Ford, S. J.; Bell, A. F.; Wilson, G.; Hecht, L.; Cooper, A. Vibrational Raman Optical-Activity of Biopolymers. *Faraday Discuss.* **1994**, *99*, 217−232.
(30) Barron, L. D.; Hecht, L.; Bell, A. F.; Wilson, G. Recent Developments in Raman Optical Activity of Biopolymers. *Appl. Spectrosc.* **1996**, *50*, 619−629.
(31) Barron, L. D.; Zhu, F.; Hecht, L. Raman Optical Activity: An Incisive Probe of Chirality, and of Biomolecular Structure and Behaviour. *Vib. Spectrosc.* **2006**, *42*, 15−24.
(32) Nafie, L. A. *Overview of Vibrational Optical Activity*; John Wiley & Sons, Ltd: Hoboken, NJ, 2011.
(33) Barron, L. D.; Gargaro, A. R.; Wen, Z. Q. Vibrational Raman Optical Activity of Peptides and Proteins. *J. Chem. Soc., Chem. Commun.* **1990**, *0*, 1034−1036.
(34) Luber, S.; Reiher, M. Raman Optical Activity Spectra of Chiral Transition Metal Complexes. *Chem. Phys.* **2008**, *346*, 212−223.
(35) Osińska, K.; Pecul, M.; Kudelski, A. Circularly Polarized Component in Surface-Enhanced Raman Spectra. *Chem. Phys. Lett.* **2010**, *496*, 86−90.
(36) Novák, V.; Šebestík, J.; Bouř, P. Theoretical Modeling of the Surface-Enhanced Raman Optical Activity. *J. Chem. Theory Comput.* **2012**, *8*, 1714−1720.
(37) Yamamoto, S.; Bouř, P. Transition Polarizability Model of Induced Resonance Raman Optical Activity. *J. Comput. Chem.* **2013**, *34*, 2152−2158.
(38) Parchaňský, V.; Kapitán, J.; Kaminský, J.; Šebestík, J.; Bouř, P. Ramachandran Plot for Alanine Dipeptide as Determined from Raman Optical Activity. *J. Phys. Chem. Lett.* **2013**, *4*, 2763−2768.
(39) Zhu, F.; Isaacs, N. W.; Hecht, L.; Barron, L. D. Raman Optical Activity: A Tool for Protein Structure Analysis. *Structure* **2005**, *13*, 1409−1419.
(40) Barron, L. D.; Hecht, L.; Blanch, E. W.; Bell, A. F. Solution Structure and Dynamics of Biomolecules from Raman Optical Activity. *Prog. Biophys. Mol. Biol.* **2000**, *73*, 1−49.
(41) Wen, Z. Q.; Hecht, L.; Barron, L. D. α-Helix and Associated Loop Signatures in Vibrational Raman Optical Activity Spectra of Proteins. *J. Am. Chem. Soc.* **1994**, *116*, 443−445.
(42) Carter, D. C.; Ho, J. X. *Structure of Serum Albumin*; Academic Press: New York, 1994.
(43) Aoki, K.; Okabayashi, H.; Maezawa, S.; Mizuno, T.; Murata, M.; Hiramatsu, K. Raman studies of Bovine Serum Albumin−Ionic Detergent Complexes and Conformational Change of Albumin Molecule induced by Detergent Binding. *Biochim. Biophys. Acta, Protein Struct. Mol. Enzymol.* **1982**, *703*, 11−16.
(44) Wei, X.; Chang, Z.; Liu, H. Influence of Sodium Dodecyl Sulfate on the Characteristics of Bovine Serum Albumin Solutions and Foams. *J. Surfactants Deterg.* **2003**, *6*, 107−112.
(45) Miura, T.; Takeuchi, H.; Harada, I. Tryptophan Raman Bands Sensitive to Hydrogen Bonding and Side-Chain Conformation. *J. Raman Spectrosc.* **1989**, *20*, 667−671.
(46) Vasilescu, M.; Angelescu, D.; Almgren, M.; Valstar, A. Interactions of Globular Proteins with Surfactants Studied with Fluorescence Probe Methods. *Langmuir* **1999**, *15*, 2635−2643.
(47) Diem, M. *Introduction to Modern Vibrational Spectroscopy*; Wiley-VCH: Weinheim, Germany; 1993.
(48) Wilson, G.; Hecht, L.; Barron, L. D. Residual Structure in Unfolded Proteins Revealed by Raman Optical Activity. *Biochemistry* **1996**, *35*, 12518−12525.
(49) Smyth, E.; Syme, C. D.; Blanch, E. W.; Hecht, L.; Vašák, M.; Barron, L. D. Solution Structure of Native Proteins with Irregular Folds from Raman Optical Activity. *Biopolymers* **2001**, *58*, 138−151.
(50) Wilson, G.; Hecht, L.; Barron, L. D. Vibrational Raman Optical Activity of α-Helical and Unordered Poly(L-lysine). *J. Chem. Soc., Faraday Trans.* **1996**, *92*, 1503−1509.
(51) McColl, I. H.; Blanch, E. W.; Hecht, L.; Barron, L. D. A Study of α-Helix Hydration in Polypeptides, Proteins, and Viruses Using

Vibrational Raman Optical Activity. *J. Am. Chem. Soc.* **2004**, *126*, 8181−8188.
(52) Jones, M. N.; Skinner, H. A.; Tipping, E. Interaction between Bovine Serum-Albumin and Surfactants. *Biochem. J.* **1975**, *147*, 229−234.
(53) Jones, M. N. *Biochemical Thermodynamics*, 2nd ed.; Elsevier: Amsterdam, The Netherlands, 1988.